Numerical Simulation Using ADI–FDTD Method to Estimate Shielding Effectiveness of Thin Conductive Enclosures

Takefumi Namiki, *Member, IEEE,* and Koichi Ito, *Member, IEEE*

***Abstract*—Numerical simulations were run using the alternating-direction implicit–finite-difference time-domain (ADI–FDTD) method to calculate the shielding effectiveness of various enclosures. The enclosures were composed of very thin conductive sheets, which are generally fabricated using conductive paints or electroless plating techniques on plastic surfaces. In this case, very fine cells must be used for finite-difference time-domain (FDTD) modeling. In the conventional FDTD method, fine cells reduce the time-step size because of the Courant–Friedrich–Levy (CFL) stability condition, which results in an increase in computational effort, such as the central processing unit (CPU) time. In the ADI–FDTD method, on the other hand, a larger time-step size than allowed by the CFL stability condition limitation can be set because the algorithm of this method is unconditionally stable. Consequently, an increase in computational efforts caused by fine cells can be prevented. The results from the ADI–FDTD method were compared with results from the conventional FDTD method, analytical solutions, and experimental data. These results clearly agree quite well, and the required CPU time for the ADI–FDTD method can be much shorter than that for the FDTD method.**

***Index Terms*—ADI–FDTD method, CFL stability condition, FDTD method, shielding effectiveness.**

I. Introduction

In RECENT years, it has become increasingly important to estimate the electromagnetic shielding effectiveness (SE) of the cases that enclose various types of electronic equipment. For optimal cost efficiency, using a numerical technique during the design phase of the equipment is indispensable for estimating the SE of various shapes and materials for these enclosures. The finite-difference time-domain (FDTD) method [1] is well known as being one of the most useful numerical techniques for such problems. However, for calculating the effectiveness of an enclosure whose thickness is much smaller than the operating wavelength, the conventional FDTD method has a disadvantage. For the FDTD modeling, very fine cells must be used in the region with thin sheets, and these fine cells reduce the time-step size because of the Courant–Friedrich–Levy (CFL) stability condition [2], which results in an increase in computational effort, such as the CPU time. In fact, several micrometer-thick thin shielding sheets, which are generally fabricated using conductive paints or electroless plating techniques on plastic surfaces, are often used today, thus, the inefficiency of the FDTD method is a very serious issue for optimizing the design process.

We previously proposed the alternating-direction implicit–finite-difference time-domain (ADI–FDTD) method for solving two-dimensional Maxwell's equations [3] and extended it to three dimensions [4]–[6]. We showed that the algorithm of the method is unconditionally stable and free from the CFL stability condition restraint. Soon after having published our findings, Zheng *et al.* reported the same approach [7] and theoretically proved the stability of the scheme in three dimensions [8].

Since the limitation on the maximum time-step size in the ADI–FDTD method is no longer dependent on the CFL stability condition, the maximum time-step size is limited by numerical errors that depend on what kinds of problems or models are calculated. On the other hand, the maximum time-step size is certainly limited by the maximum frequency of the pulse spectrum, in accordance with the Nyquist sampling theorem, when the broad-band frequency characteristics are calculated by applying a Fourier transformation to the impulse response of the time-domain simulation. However, this limitation is not very strict, especially if the frequency in question is not relatively very high.

In this paper, we propose using the ADI–FDTD method to solve the above shielding problems. The characteristics of the SE of various enclosures are calculated using the ADI–FDTD method, and the results for this method are compared with results for the conventional FDTD method, experimental data, and analytical solutions. This research is intended to be applied for recent high-speed digital electronic equipment, thus, the examined frequency bandwidth is set to about 100 MHz–1 GHz. In Sections II and III, two-dimensional problems are discussed, and inSection IV, three-dimensional problems are discussed.

II. Shielding of Plane Wave by Thin Metal Sheet

A. Numerical Modeling

Before analyzing enclosures, simple plane sheets are examined. Fig. 1 shows a two-dimensional FDTD model that includes a thin metal sheet to shield plane waves. For the sake of explanation, the figure scale of the numerical model shown here is different from that of the real model. Two electric-field components (E_x and E_y) and one magnetic-field component (H_z) are arranged on the cells in the computational domain. Mur's first-order absorbing boundary conditions (ABCs) [9] are set at

Manuscript received June 28, 2000; revised September 28, 2000.

T. Namiki is with the Computational Science and Engineering Center, Fujitsu Ltd., Chiba 261-8588, Japan (e-mail: namiki@strad.se.fujitsu.co.jp).

K. Ito is with the Faculty of Engineering, Department of Urban Environment Systems, Chiba University, Chiba 263-8522, Japan (e-mail: ito@cute.te.chiba-u.ac.jp).

Publisher Item Identifier S 0018-9480(01)03993-X.

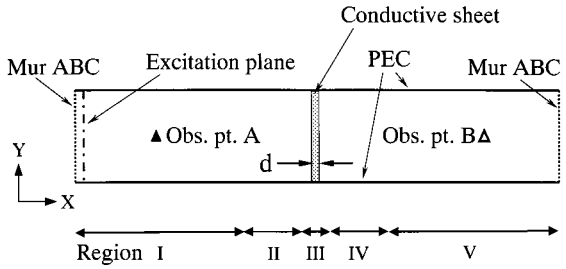

Fig. 1. Numerical model of thin metal sheet to shield plane wave.

TABLE I
(a) SPATIAL DISCRETIZATION OF COPPER SHEET MODEL. (b) SPATIAL DISCRETIZATION OF IRON SHEET MODEL

	Region				
	I	II	III	IV	V
ΔX	0.5 mm	0.5 mm - 0.5 μm	0.5 μm	0.5 μm - 0.5 mm	0.5 mm
ΔX(i+1) / ΔX(i)	1.0	0.1	1.0	10.0	1.0
Number of ΔX	142	4	18	4	142
ΔY	0.5 mm				
ΔY(j+1) / ΔY(j)	1.0				
Number of ΔY	21				

(a)

	Region				
	I	II	III	IV	V
ΔX	0.1 mm	0.1 mm - 0.1 μm	0.1 μm	0.1 μm - 0.1 mm	0.1 mm
ΔX(i+1) / ΔX(i)	1.0	0.1	1.0	10.0	1.0
Number of ΔX	137	4	28	4	137
ΔY	0.1 mm				
ΔY(j+1) / ΔY(j)	1.0				
Number of ΔY	21				

(b)

the x-directional terminals of the domain, and perfect electric conductor (PEC) boundary conditions are set at the y-directional terminals of the domain. Numerical simulations are carried out for two kinds of sheets. One is a 4-μm-thick copper sheet with a relative permittivity of 1.0, relative permeability of 1.0, and conductivity of 5.8×10^7 S/m. The other is a 2-μm-thick iron sheet with a relative permittivity of 1.0, relative permeability of 140.0, and conductivity of 0.986×10^7 S/m. Uniform cells are used in the y-direction, and nonuniform cells are used in the x-direction, to treat both the thin sheets and horizontally wide computational region. In addition, Δx around the metal sheet region is set sufficiently smaller than the minimum skin depth of the metal at the maximum frequency required for the examination. Table I(a) and (b) describes the spatial discretization of the copper and iron sheets, respectively. In the copper sheet model, the conductive sheet region is divided into eight cells, and the minimum cell size is 0.5 μm$\times$ 0.5 mm. Therefore, the CFL stability condition of this model is $\Delta t \leq 1.66666$ fs. In the iron sheet model, the conductive sheet region is divided into 20 cells, and the minimum cell size is 0.1 μm$\times$ 0.1 mm. The

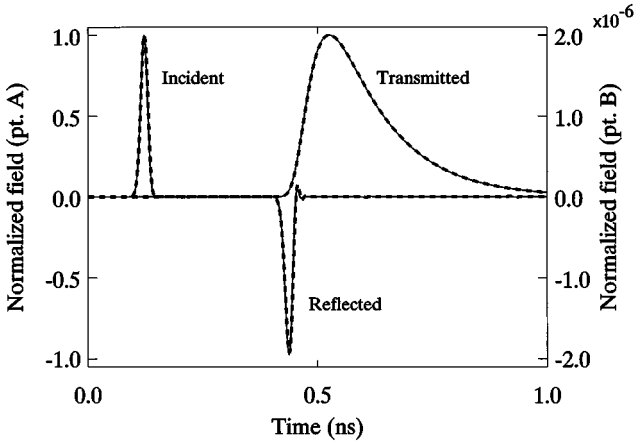

(a)

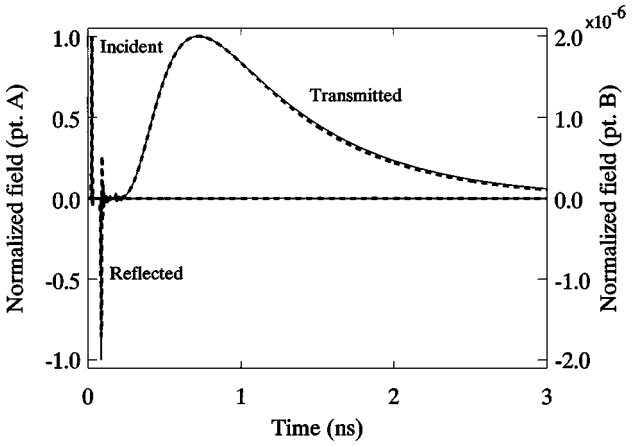

(b)

Fig. 2. (a) Normalized electric field versus time of copper sheet mode. (b) Normalized electric field versus time of iron sheet model. (Solid line: conventional FDTD, dashed line: ADI–FDTD.)

CFL stability condition of this model is $\Delta t \leq 0.33333$ fs. The time-step size for the conventional FDTD method is set so as to satisfy the CFL stability condition, and the time-step size for the ADI–FDTD method is set much larger than the previous size. A Gaussian pulse is applied at the E_y components on the excitation plane, and the E_y components at observation points A and B are output. The waveform of the applied pulse is as follows:

$$E_y(t) = E_0 \exp\left[\frac{-(t-t_0)^2}{T^2}\right],$$
$$t_0 = 40.0 \text{ ps}; \quad T = 10.7 \text{ ps}.$$

B. Numerical Results

Fig. 2 shows the observed electric fields, which are normalized by the value of the incident pulse amplitude. Incident and reflected pulses are observed at point A and a transmitted pulse is observed at point B. The numerical results for the ADI–FDTD method and for the conventional FDTD method agree quite well. The transmitted pulse drags a long tail in the time domain because of multireflections in the metal sheet region, thus, the number of time-loop iterations that should be done in the numerical calculation is dependent on this tail. The SE values are calculated by applying a Fourier transformation

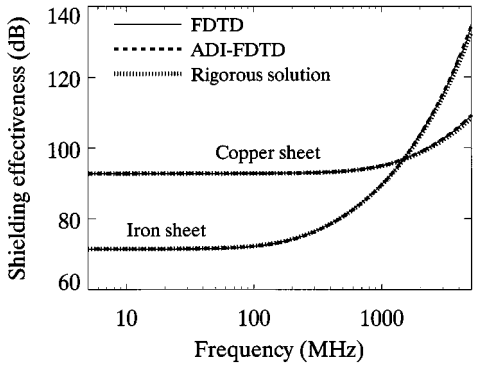

Fig. 3. SE versus frequency of Fig. 1 model (solid line: conventional FDTD, dashed line: ADI–FDTD, dotted line: rigorous solution[10]).

TABLE II
(a) TIME-STEPPING MODELING AND COMPUTATIONAL EFFORT FOR THE SIMULATION OF COPPER SHEET MODEL. (b) TIME-STEPPING MODELING AND COMPUTATIONAL EFFORT FOR THE SIMULATION OF IRON SHEET MODEL

	Time-step size	Time-loop iterations	CPU time	Memory
ADI-FDTD	665 fs	2255	5 s	1.52 Mb
FDTD	1.66 fs	903600	513 s	1.02 Mb

(a)

	Time-step size	Time-loop iterations	CPU time	Memory
ADI-FDTD	665 fs	12030	28 s	2.00 Mb
FDTD	0.33 fs	24242424	13700 s	1.50 Mb

(b)

to the incident and transmitted pulses. Fig. 3 shows these SE values with rigorous solutions derived by Schelkunoff's theory [10]. The numerical results from the ADI–FDTD method, the conventional FDTD method, and the rigorous solution clearly agree quite well. Table II lists the required computational effort for these simulations, along with information about their time-stepping modeling. All calculations in this paper were performed on an Ultra SPARC II 360-MHz workstation. Since the time-step size for the ADI–FDTD method can be set about 400 or 2000 times larger than that for the conventional FDTD method, the CPU time for the ADI–FDTD method can be reduced to about 1.0% or 0.2% of that for the conventional FDTD method while maintaining the same level of accuracy.

III. SHIELDING EFFECTIVENESS OF TWO-DIMENSIONAL CONDUCTIVE ENCLOSURE

A. Numerical Modeling

Fig. 4 shows a two-dimensional FDTD model that includes a square enclosure composed of thin conductive sheets to shield the electromagnetic field excited by a small electric dipole. The electromagnetic-field components are arranged in the same way as the previous model. Mur's ABC is applied at all outer surfaces of the computational domain. The enclosure is a 0.015-mm-thick conductive sheet with a relative permittivity of 1.0, relative permeability of 1.0, and conductivity of 1.0×10^3 S/m. Table III describes the x-directional spatial discretization of a quarter region of the domain. The model is clearly

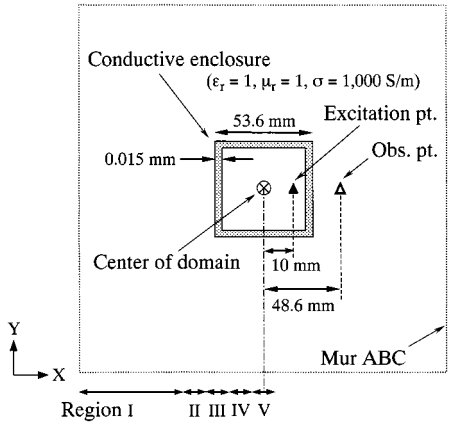

Fig. 4. Numerical model of square enclosure composed of thin conductive sheets to shield field excited by two-dimensional dipole.

TABLE III
SPATIAL DISCRETIZATION OF FIG. 4 MODEL

	Region				
	I	II	III	IV	V
ΔX	8.0 mm	8.0 mm - 5.0 μm	5.0 μm	5.0 μm - 0.625 mm	1.0 mm
ΔX(i+1) / ΔX(i)	1.0	1.0 - 0.2	1.0	5.0	1.0
Number of ΔX	57	38	5	4	51

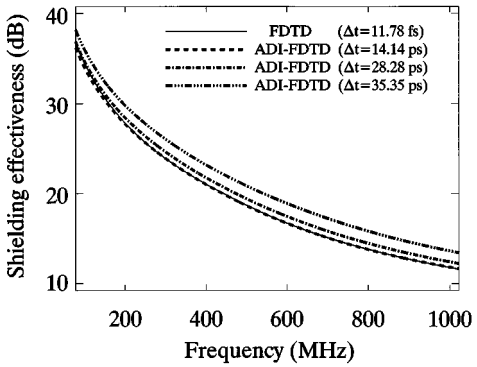

Fig. 5. SE versus frequency of Fig. 4 model (solid line: conventional FDTD, other lines: ADI–FDTD with different time-step sizes).

TABLE IV
TIME-STEPPING MODELING AND COMPUTATIONAL EFFORT FOR THE SIMULATION OF FIG. 4 MODEL

	Time-step size	Time-loop iterations	CPU time	Memory
ADI-FDTD	14.14 ps	212	4.6 s	4.21 Mb
FDTD	11.78 fs	254669	1191 s	2.70 Mb

symmetrical with respect to the center of the domain; therefore, the spatial discretization of the domain is also set symmetrically. The conductive sheet region is divided into three cells, and the minimum cell size is 0.005×0.005 mm^2. Therefore, the CFL stability condition of this model is $\Delta t \leq 11.7851$ fs. The time-step size for the conventional FDTD method is set so as to satisfy the CFL stability condition, and the time-step size for the ADI–FDTD method is set much larger than the previous size. A physical time for each simulation, which is a product

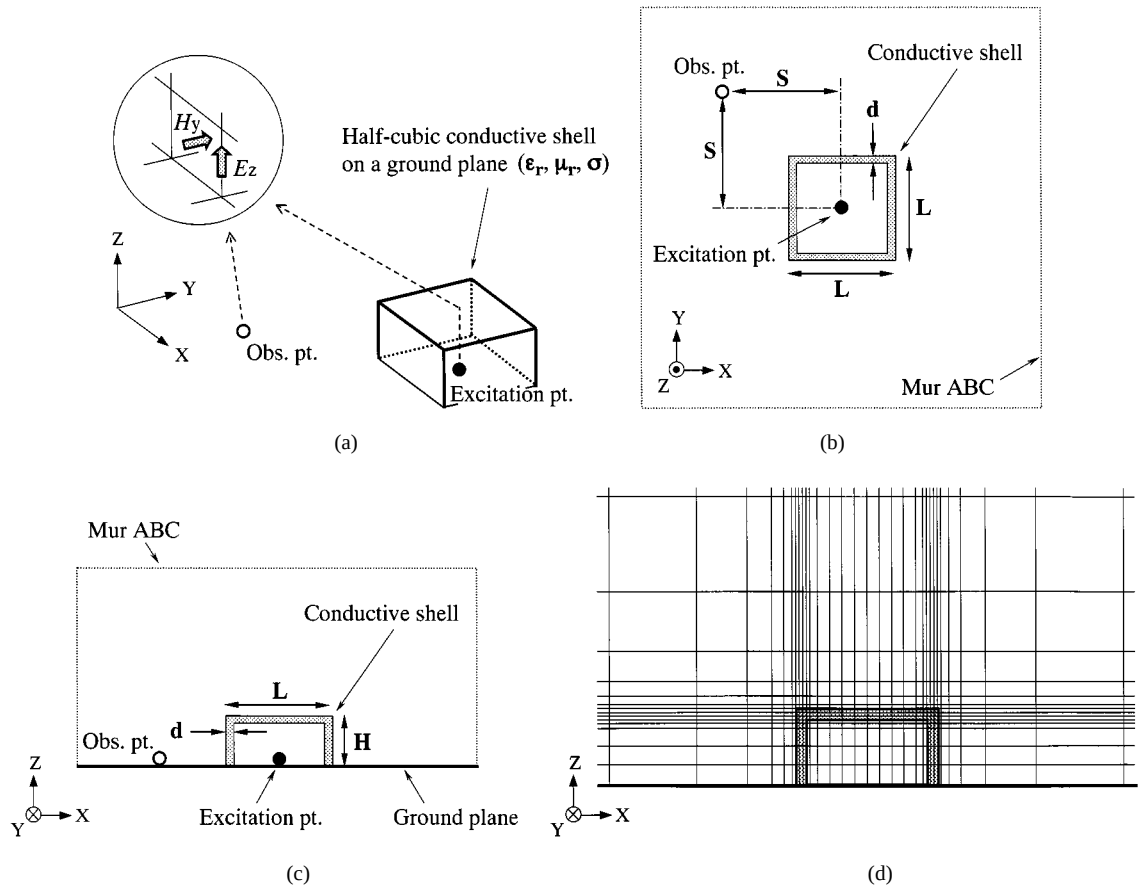

Fig. 6. Numerical model consists of half-cubic conductive shell on ground plane. (a) Bird's-eye view. (b) Top view. (c) Side view. (d) Spatial discretization of half-cubic conductive shell model (side view).

of the time-step size and the number of time-loop iterations, must be about 3.0 ns for the oscillation of the output pulse to converge.

A partial Gaussian pulse is applied to the E_y component at the excitation point, and the E_y component at the observation point is output. The waveform of the applied pulse is as follows:

$$E_y(t) = E_y(t) + E_0(t - t_0)\exp\left[\frac{-(t-t_0)^2}{T^2}\right],$$
$$t_0 = 0.4\,\text{ns}; \quad T = 0.106\,\text{ns}.$$

Numerical simulations are performed twice, with and without the enclosure. The SE values are calculated by applying a Fourier transformation to each output field.

B. Numerical Results

Fig. 5 shows the SE values calculated by the conventional FDTD method and the ADI–FDTD method, which is performed with different time-step sizes. Increasing the time-step size increases the numerical error. However, the numerical results for the ADI–FDTD method performed with $\Delta t = 14.14$ ps and those for the conventional FDTD method performed with $\Delta t = 11.78$ fs agree quite well. Table IV lists the computational effort and time-stepping modeling parameters for this simulation. The time-step size for the ADI–FDTD method can be set about 1200 times larger than that for the conventional FDTD method. The CPU time for the ADI–FDTD method can thereby be reduced to about 0.4% of that for the conventional FDTD method while maintaining the same level of accuracy.

TABLE V
THREE TYPES OF HALF-CUBIC CONDUCTIVE SHELLS

	L (mm)	H (mm)	d (mm)	S (mm)	μr	εr	σ (S/m)
Type-1	40.0	18.0	3.0	81.0	1.0	1.0	2.3
Type-2	56.0	25.0	0.375	92.0	1.0	1.0	40.0
Type-3	56.0	25.0	0.024	92.0	1.0	1.0	2400

IV. Shielding Effectiveness of Three-Dimensional Conductive Enclosures

A. Numerical Modeling

Fig. 6 shows a three-dimensional FDTD model for estimating SE. It consists of a half-cubic conductive shell on a ground plane. The numerical simulations are performed in the same way as for the previous two-dimensional models. Nonuniform cells are used to treat both the thin sheets of the shell and a wide computational region. A partial Gaussian pulse is applied at the excitation point, and the field at the observation point is output. The waveform of the applied pulse is as follows:

$$E_y(t) = E_y(t) + E_0(t - t_0)\exp\left[\frac{-(t-t_0)^2}{T^2}\right],$$
$$t_0 = 2.15\,\text{ns}; \quad T = 0.576\,\text{ns}.$$

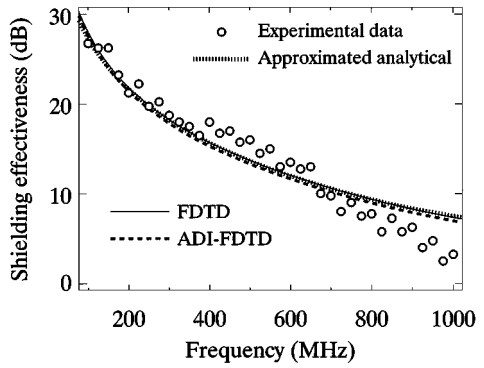

(a)

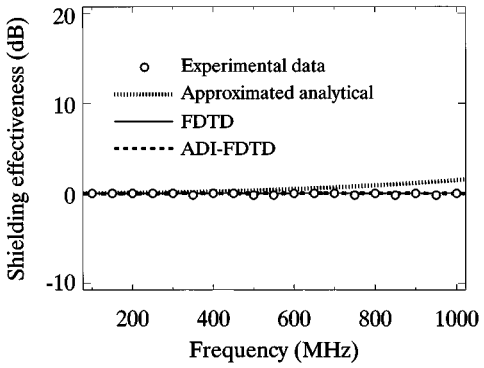

(b)

Fig. 7. (a) SE for electric field of type-1 model. (b) SE for magnetic field of type-1 model. (Solid line: conventional FDTD, dashed line: ADI–FDTD, dotted line: approximated analytical solution [12], [13] for equivalent radius of 26.7 mm, circular symbol: experimental data [11].)

Numerical calculations are carried out two times, with and without the shell. The SE values are calculated by applying a Fourier transformation to each output field. To estimate the electric-field SE, vertical electric-field components are used for excitation and observation. To estimate the magnetic-field SE, horizontal magnetic-field components are used rather than vertical electric-field components. Mur's ABC is applied at all outer surfaces of the computational domain, except the bottom ground plane. The SE values are calculated for three types of shells, which Table V describes in greater detail, using the ADI–FDTD method and the conventional FDTD method. These results are compared with experimental data and analytical solutions.

The experimental data is derived from [11]. To measure the electric-field SE, small dipole antennas were placed at the excitation point as the source and at the observation point as the detector. Instead of dipole antennas, small loop antennas were used to measure the magnetic-field SE. The approximated analytical solutions are calculated using formulas from [12] and [13]. The SE values for the electric and magnetic fields of a conductive spherical shell of arbitrary size can be estimated by this theory. To adapt this theory to the cubic shell shown in Fig. 6, a sphere with an inner surface area equivalent to the external surface area of the cubic shell is considered. The equivalent radius indicates the radius of this sphere. The thickness of the spherical shell is the same as that of the cubic one.

TABLE VI
TIME-STEPPING MODELING AND COMPUTATIONAL EFFORT FOR THE SIMULATION OF TYPE-1 MODEL

	Time-step size	Time-loop iterations	CPU time	Memory
ADI-FDTD	19.2 ps	360	103 s	20.3 Mb
FDTD	1.92 ps	3600	227 s	10.6 Mb

TABLE VII
TIME-STEPPING MODELING AND COMPUTATIONAL EFFORT FOR THE SIMULATION OF TYPE-2 MODEL

	Time-step size	Time-loop iterations	CPU time	Memory
ADI-FDTD	9.60 ps	720	373 s	35.4 Mb
FDTD	0.24 ps	28800	3791 s	18.4 Mb

TABLE VIII
TIME-STEPPING MODELING AND COMPUTATIONAL EFFORT FOR THE SIMULATION OF TYPE-3 MODEL

	Time-step size	Time-loop iterations	CPU time	Memory
ADI-FDTD	0.96 ps	7200	3749 s	35.6 Mb
FDTD	15.38 fs	449415	60060 s	18.4 Mb

B. Numerical Results

Fig. 7 shows the SE values for electric and magnetic fields for a type-1 shell. The numerical results for the ADI–FDTD and conventional FDTD agree quite well. Moreover, they correspond with the approximated analytical solution and are quite similar to the experimental data. In the type-1 model, the 3-mm-thick conductive shell region is divided into three cells, thus, the minimum cell size is $1.0 \times 1.0 \times 1.0$ mm^3. Therefore, the CFL stability condition of this model is $\Delta t \leq 1.9245$ ps. Table VI lists the computational effort and time-stepping modeling parameters. The time-step size for the conventional FDTD method is set so as to satisfy the CFL stability condition, and the time-step size for the ADI–FDTD method can be set ten times larger than the previous size. Consequently, the required CPU time for the ADI–FDTD method is reduced to 47% of that for the conventional FDTD method.

Fig. 8(a) shows the SE values for an electric field for a type-2 shell. The numerical results from the ADI–FDTD method, conventional FDTD method, and approximated analytical solution all agree quite well. Fig. 8(b) shows the SE values for a magnetic field for a type-2 shell. The numerical results from the ADI–FDTD method and the approximated analytical solution agree well. However, for reasons that are unclear, the numerical results from the conventional FDTD method are obviously abnormal. In the type-2 model, the 0.375-mm-thick conductive shell region is divided into three cells, thus, the minimum cell size is $0.125 \times 0.125 \times 0.125$mm^3. Therefore, the CFL stability condition of this model is $\Delta t \leq 0.24056$ ps. Table VII lists the computational effort and time-stepping modeling parameters. The time-step size for the ADI–FDTD method is set 40 times larger than the previous size. Consequently, the required CPU time for the ADI–FDTD method is reduced to 9.8% of that for the conventional FDTD method.

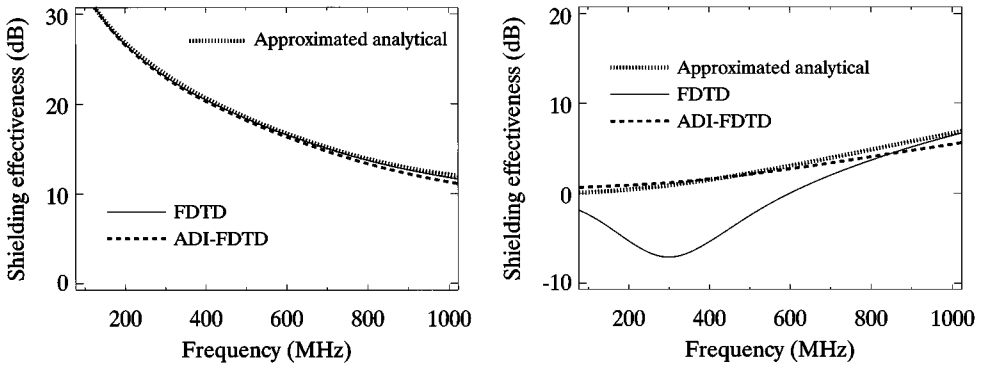

Fig. 8. (a) SE for electric field of type-2 model. (b) SE for magnetic field of type-2 model. (Solid line: conventional FDTD, dashed line: ADI–FDTD, dotted line: approximated analytical solution for equivalent radius of 37.3 mm.)

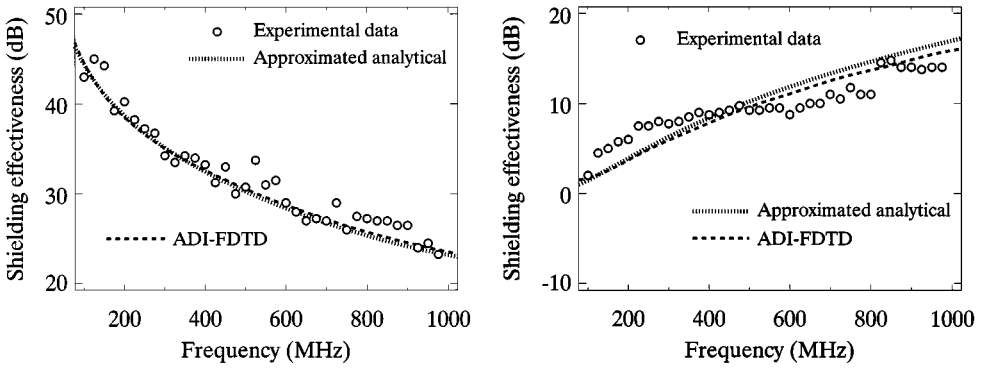

Fig. 9. (a) SE for electric field of type-3 model. (b) SE for magnetic field of type-3 model. (Dashed line: ADI–FDTD, dotted line: approximated analytical solution for equivalent radius of 37.3 mm, circular symbols: experimental data [11].)

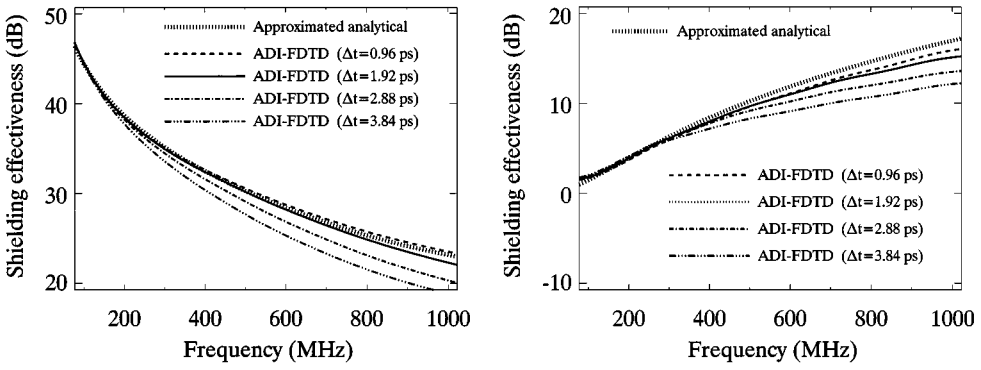

Fig. 10. (a) SE for electric field of type-3 model. (b) SE for magnetic field of type-3 model. (Dotted line: approximated analytical solution for equivalent radius of 37.3 mm, other lines: ADI–FDTD with different time-step sizes.)

Fig. 9 shows the SE values for electric and magnetic fields for a type-3 shell. The numerical results for the ADI–FDTD method and approximated analytical solution agree quite well. Moreover, they are quite similar to the experimental data. There are no results for the conventional FDTD method here because ordinary calculations cannot be done for this model if the conventional FDTD method is used. The reason is as follows. Since the time-step size is very small, the applied pulse is excited over very long time periods, and its amplitude grows very slowly. In this case, the pulse does not correctly propagate in the computational domain. To prevent that, a pulse with a short width in the time-domain must be used. However, such a pulse includes a frequency component so high that the maximum cell size in the computational domain must become much smaller, which results in a significant increase in computational effort. In the type-3 model, the 0.024-mm-thick conductive shell region is divided into three cells, thus, the minimum cell size is $0.008 \times 0.008 \times 0.008\ \text{mm}^3$. Therefore, the CFL stability condition of this model is $\Delta t \leq 15.396$ fs. Although numerical results cannot be obtained by the conventional FDTD method, Table VIII lists the estimated computational effort for the two methods. The time-step size for the ADI–FDTD method is set 62

times larger than that for the conventional FDTD method. Consequently, the required CPU time for the ADI–FDTD method is reduced to 6.2% of that for the conventional FDTD method.

Fig. 10 shows the SE values for a type-3 shell calculated by the ADI–FDTD method, which is performed with different time-step sizes. Increasing the time-step size increases the numerical error, and the error is substantial at higher frequencies. The reason is probably that the phase velocity of an electromagnetic wave is faster at a higher frequency in a lossy medium. In other words, in shielding problems, the maximum time-step size is limited by the velocity of an electromagnetic wave in the conductive sheet region.

V. Conclusion

Numerical simulations using the ADI–FDTD method have been presented for solving the shielding problems of various enclosures composed of thin conductive sheets. These numerical results were compared with those from the conventional FDTD method, analytical solutions, and experimental data. The results agree quite well, except for some incorrect numerical results from the conventional FDTD method. The ADI–FDTD method guarantees a stable calculation with any time-step size, and a large time-step size reduces both the number of time-loop iterations and the required CPU time for the calculation. The required CPU time for the ADI–FDTD method is clearly much shorter than that for the conventional FDTD method. The ADI–FDTD method is an efficient and accurate numerical technique for estimating the SE when designing shielding for electronic equipment.

References

[1] K. S. Yee, "Numerical solution of initial boundary value problems involving Maxwell's equations in isotropic media," *IEEE Trans. Antennas Propagat.*, vol. AP-14, pp. 302–307, May 1966.

[2] A. Taflove, *Computational Electrodynamics*. Norwood, MA: Artech House, 1995.

[3] T. Namiki, "A new FDTD algorithm based on alternating-direction implicit method," *IEEE Trans. Microwave Theory Tech.*, vol. 47, pp. 2003–2007, Oct. 1999.

[4] T. Namiki and K. Ito, "A study of numerical simulation of transmission line using ADI–FDTD method," (in Japanese), IEICE, Tokyo, Japan, Tech. Rep., vol. MW98–83, pp. 57–63, Sept. 1998.

[5] ——, "The electromagnetic simulation system based on the FDTD method for practical use," presented at the Asia–Pacific Microwave Conf., Yokohama, Japan, Dec. 1998.

[6] ——, "3-D ADI–FDTD method—Unconditionally stable time-domain algorithm for solving full vector Maxwell's equations," *IEEE Trans. Microwave Theory Tech.*, vol. 48, pp. 1743–1748, Oct. 2000.

[7] F. Zheng, Z. Chen, and J. Zhang, "A finite-difference time-domain method without the courant stability condition," *IEEE Microwave Guided Wave Lett.*, vol. 9, pp. 441–443, Nov. 1999.

[8] ——, "Toward the development of a three-dimensional unconditionally stable finite-difference time-domain method," *IEEE Trans. Microwave Theory Tech.*, vol. 48, pp. 1550–1558, Sept. 2000.

[9] G. Mur, "Absorbing boundary conditions for the finite-difference approximation of the time-domain electromagnetic field equations," *IEEE Trans. Electromagn. Compat.*, vol. EMC-23, pp. 377–382, Nov. 1981.

[10] S. A. Schelkunoff, *Electromagnetic Waves*. New York: Van Nostrand, 1943.

[11] H. Isono, K. Saegusa, and N. Hase, "A simple calculation method for estimating shielding effectiveness of conducting spherical cell" (in Japanese), *Trans. IEICE*, vol. J82-B, no. 2, pp. 302–307, Feb. 1999.

[12] C. W. Harrison and C. H. Papas, "On the attenuation of transient fields by imperfectly conducting spherical shells," *IEEE Trans. Antennas Propagat.*, vol. AP-13, no. 6, pp. 960–966, Nov. 1965.

[13] N. Hase and K. Kobayashi, "A method of measuring shielding effectiveness for conducting materials using a spherical cell" (in Japanese), *Trans. IEICE*, vol. J70-B, no. 7, pp. 862–873, July 1987.

Takefumi Namiki (M'99) was born in Chiba, Japan, on January 24, 1963. He received the B.S. degree in physics from Tohoku University, Sendai, Japan, in 1985, and the D.E. degree in electrical engineering from Chiba University, Chiba, Japan, in 2001.

From 1986 to 1991, he was with Fujitsu Laboratories Ltd., Atsugi, Japan, where he was engaged in research of high-speed optical modulator for optical communications systems. In 1991, he joined Fujitsu Ltd., Tokyo, Japan, where he was engaged in research and development of the computational science. Since 1994, he has been engaged in research of computational electromagnetics with Fujitsu Ltd. His research interests include numerical techniques for modeling electromagnetic fields and waves, and the computer-aided engineering (CAE) system of microwave circuits, antennas, and optical waveguides.

Dr. Namiki is a member of the Institute of Electrical, Information and Communication Engineers (IEICE), Japan.

Koichi Ito (M'81) was born in Nagoya, Japan, on June 4, 1950. He received the B.S. and M.S. degrees from Chiba University, Chiba, Japan, in 1974 and 1976, respectively, and the D.E. degree from the Tokyo Institute of Technology, Tokyo, Japan, in 1985, all in electrical engineering.

From 1976 to 1979, he was a Research Associate at the Tokyo Institute of Technology. From 1979 to 1989, he was a Research Associate at Chiba University. From 1989 to 1997, he was an Associate Professor in the Department of Electrical and Electronics Engineering, Chiba University. He is currently a Professor in the Department of Urban Environment Systems, Chiba University. In 1989, 1994, and 1998, he was an Invited Professor at the Universite de Rennes I, Rennes, France. His main interests include analysis and design of printed antennas and small antennas, research on evaluation of the interaction between electromagnetic fields and the human body, and antennas for medical applications of microwaves.

Dr. Ito is a member of the American Association for the Advancement of Science (AAAS), the Institution of Electrical, Information and Communication Engineers (IEICE), Japan, the Institute of Image Information and Television Engineers of Japan, and the Japanese Society of Hyperthermic Oncology.